

Measurement of the branching ratio

$$\mathcal{B}(D^+ \rightarrow \rho^0 \ell^+ \nu_\ell) / \mathcal{B}(D^+ \rightarrow \bar{K}^{*0} \ell^+ \nu_\ell)$$

E. M. Aitala,⁹ S. Amato,¹ J. C. Anjos,¹ J. A. Appel,⁵ D. Ashery,¹⁵ S. Banerjee,⁵
I. Bediaga,¹ G. Blaylock,⁸ S. B. Bracker,¹⁶ P. R. Burchat,¹⁴ R. A. Burnstein,⁶ T. Carter,⁵
H. S. Carvalho,¹ N. K. Coptý,¹³ L. M. Cremaldi,⁹ C. Darling,¹⁹ K. Denisenko,⁵
A. Fernandez,¹² P. Gagnon,² K. Gounder,⁹ A. M. Halling,⁵ G. Herrera,⁴ G. Hurvits,¹⁵
C. James,⁵ P. A. Kasper,⁶ S. Kwan,⁵ D. C. Langs,¹¹ J. Leslie,² B. Lundberg,⁵
S. May-Tal-Beck,¹⁵ B. Meadows,³ J. R. T. de Mello Neto,¹ R. H. Milburn,¹⁷
J. M. de Miranda,¹ A. Napier,¹⁷ A. Nguyen,⁷ A. B. d'Oliveira,^{3,12} K. O'Shaughnessy,²
K. C. Peng,⁶ L. P. Perera,³ M. V. Purohit,¹³ B. Quinn,⁹ S. Radeztsky,¹⁸ A. Rafatian,⁹
N. W. Reay,⁷ J. J. Reidy,⁹ A. C. dos Reis,¹ H. A. Rubin,⁶ A. K. S. Santha,³
A. F. S. Santoro,¹ A. J. Schwartz,¹¹ M. Sheaff,¹⁸ R. A. Sidwell,⁷ A. J. Slaughter,¹⁹
M. D. Sokoloff,³ N. R. Stanton,⁷ K. Stenson,¹⁸ D. J. Summers,⁹ S. Takach,¹⁹ K. Thorne,⁵
A. K. Tripathi,¹⁰ S. Watanabe,¹⁸ R. Weiss-Babai,¹⁵ J. Wiener,¹¹ N. Witchey,⁷ E. Wolin,¹⁹
D. Yi,⁹ S. Yoshida,⁷ R. Zaliznyak,¹⁴ and C. Zhang⁷

(Fermilab E791 Collaboration)

¹ *Centro Brasileiro de Pesquisas Físicas, Rio de Janeiro, Brazil*

² *University of California, Santa Cruz, California 95064*

³ *University of Cincinnati, Cincinnati, Ohio 45221*

⁴ *CINVESTAV, Mexico*

⁵ *Fermilab, Batavia, Illinois 60510*

⁶ *Illinois Institute of Technology, Chicago, Illinois 60616*

⁷ *Kansas State University, Manhattan, Kansas 66506*

⁸ *University of Massachusetts, Amherst, Massachusetts 01003*

⁹ *University of Mississippi, University, Mississippi 38677*

¹⁰ *The Ohio State University, Columbus, Ohio 43210*

¹¹ *Princeton University, Princeton, New Jersey 08544*

¹² *Universidad Autonoma de Puebla, Mexico*

¹³ *University of South Carolina, Columbia, South Carolina 29208*

¹⁴ *Stanford University, Stanford, California 94305*

¹⁵ *Tel Aviv University, Tel Aviv, Israel*

¹⁶ *317 Belsize Drive, Toronto, Canada*

¹⁷ *Tufts University, Medford, Massachusetts 02155*

¹⁸ *University of Wisconsin, Madison, Wisconsin 53706*

¹⁹ *Yale University, New Haven, Connecticut 06511*

(November 21, 2018)

Abstract

We report a measurement of the branching ratio $\mathcal{B}(D^+ \rightarrow \rho^0 \ell^+ \nu_\ell) / \mathcal{B}(D^+ \rightarrow \bar{K}^{*0} \ell^+ \nu_\ell)$ from the Fermilab charm hadroproduction experiment E791. Based on signals of 49 ± 17 events in the $D^+ \rightarrow \rho^0 e^+ \nu_e$ mode and 54 ± 18 events in the $D^+ \rightarrow \rho^0 \mu^+ \nu_\mu$ mode, we measure

$$\mathcal{B}(D^+ \rightarrow \rho^0 e^+ \nu_e) / \mathcal{B}(D^+ \rightarrow \bar{K}^{*0} e^+ \nu_e) = 0.045 \pm 0.014 \pm 0.009, \text{ and}$$

$$\mathcal{B}(D^+ \rightarrow \rho^0 \mu^+ \nu_\mu) / \mathcal{B}(D^+ \rightarrow \bar{K}^{*0} \mu^+ \nu_\mu) = 0.051 \pm 0.015 \pm 0.009.$$

Combining the results from both the electronic and muonic modes, we obtain

$$\mathcal{B}(D^+ \rightarrow \rho^0 \ell^+ \nu_\ell) / \mathcal{B}(D^+ \rightarrow \bar{K}^{*0} \ell^+ \nu_\ell) = 0.047 \pm 0.013.$$

This result is compared to theoretical predictions.

13.20.-v, 13.20.Fc, 13.30.Ce

Typeset using REVTeX

Semileptonic charm decays are useful in probing the dynamics of hadronic currents since the Cabibbo-Kobayashi-Maskawa matrix elements for the charm sector are well-known from unitarity constraints. Form factors for Cabibbo-suppressed (CS) $c \rightarrow d$ semileptonic decays can be related via Heavy Quark Effective Theory (HQET) to those for $b \rightarrow u$ semileptonic decays at the same four-velocity transfer [1]. Since knowledge of the form factors in $b \rightarrow u$ transitions is vital for extracting V_{ub} from $b \rightarrow u$ semileptonic decays in a model-independent way, study of $c \rightarrow d$ semileptonic decays can improve our knowledge of V_{ub} . Although considerable progress has been made in studying CS semileptonic charm decays to pseudoscalar mesons [2], the only previous result on CS semileptonic charm decay to a vector meson is based on four $D^+ \rightarrow \rho^0 \mu^+ \nu_\mu$ events [3]. In this Letter, we report a new measurement from the Fermilab hadroproduction experiment E791 of $\mathcal{B}(D^+ \rightarrow \rho^0 \ell^+ \nu_\ell) / \mathcal{B}(D^+ \rightarrow \bar{K}^{*0} \ell^+ \nu_\ell)$ based on more than 100 $D^+ \rightarrow \rho^0 \ell^+ \nu_\ell$ decays in the combined electronic and muonic modes.

The E791 experiment [4] recorded 2×10^{10} events from 500 GeV/ c π^- interactions in five thin targets (one platinum, four diamond) separated by gaps of 1.34 to 1.39 cm. Precision tracking and vertexing information was provided by 23 silicon microstrip detectors (6 upstream and 17 downstream of the targets) and 35 drift chamber planes. Momentum was measured with two dipole magnets. Two segmented threshold Čerenkov counters provided π/K separation in the 6 – 60 GeV/ c momentum range [5].

Candidates for $D^+ \rightarrow \rho^0 \ell^+ \nu_\ell$, $\rho^0 \rightarrow \pi^+ \pi^-$ and $D^+ \rightarrow \bar{K}^{*0} \ell^+ \nu_\ell$, $\bar{K}^{*0} \rightarrow K^- \pi^+$ decays (charge-conjugate states are implied throughout this Letter) are selected by requiring a three-prong decay vertex of charge ± 1 with one of the decay particles being identified as a lepton. A segmented lead and liquid-scintillator calorimeter [6] is used to identify the electrons, based on energy deposition and transverse shower shape. The probability that a π (K) is misidentified as an electron is about 0.8% (0.5%). Muon identification is provided by two planes of scintillation counters oriented horizontally and vertically, located behind shielding with a thickness equivalent to 2.5 meters of steel (15 interaction lengths). All the muon candidates are required to have momentum greater than 12 GeV/ c to reduce background from decays in flight. The probability that a π (K) is misidentified as a μ is

about 1.6% (2.4%).

Once the lepton is identified, the other two tracks in the vertex (h_1, h_2) are assigned hadron masses. We define the right-sign (RS) sample as vertices in which the lepton and D^+ candidate have the same charge; h_1 and h_2 are then oppositely-charged. For $D^+ \rightarrow \bar{K}^{*0} \ell^+ \nu_\ell$ candidates the hadron with odd charge is assigned a kaon mass, while for $D^+ \rightarrow \rho^0 \ell^+ \nu_\ell$ candidates h_1 and h_2 are both assigned pion masses. The RS sample contains both signal and backgrounds from reconstruction errors and other charm decay channels. The wrong-sign (WS) sample, in which the lepton and D^+ candidate have opposite charge and h_1, h_2 have like charge, provides an estimate of the shape of the background under the ρ^0 (K^{*0}) peak in the RS sample. Both kaon-assignment hypotheses are kept for WS $D^+ \rightarrow \bar{K}^{*0} \ell^+ \nu_\ell$ candidates.

Due to the undetected neutrino in the D^+ decay, there are two solutions for the D^+ momentum. We choose the lower-momentum solution since Monte Carlo studies show that, for the D^+ three-prong semileptonic decays, this solution has a slightly larger probability to be correct and offers somewhat better D^+ momentum resolution.

To minimize systematic uncertainties, most selection criteria for $D^+ \rightarrow \rho^0 \ell^+ \nu_\ell$ are identical to those for $D^+ \rightarrow \bar{K}^{*0} \ell^+ \nu_\ell$; exceptions are discussed below. In addition, all criteria except those for lepton identification are identical for electronic and muonic decays. The common criteria are the following. A decay vertex must be separated from the production vertex by at least $20\sigma_l$, where σ_l is the error on the measured separation. The decay vertex is required to be at least $5\sigma_m$ outside the nearest solid material, where σ_m is the error on the measured distance. The proper decay time for the D^+ candidate is required to be less than 5 ps. The hadron candidates in the decay are required to have momenta greater than $6 \text{ GeV}/c$. The minimum kinematically-allowed parent mass for the candidate $D^+ \rightarrow h_1 h_2 \ell \nu_\ell$ decay, $M_{min}(h_1 h_2 \ell \nu_\ell) = p_T + \sqrt{p_T^2 + M_{vis}^2}$, is required to lie between 1.6 and $2.0 \text{ GeV}/c^2$, where p_T is the transverse momentum of $h_1 h_2 \ell$ with respect to the D^+ flight direction and M_{vis} is the invariant mass of $h_1 h_2 \ell$. When masses are correctly assigned, the M_{min} distribution has a cusp at the D^+ mass. This distribution is broadened and shifted to lower mass

if there are additional neutral hadrons in the final state. The potential feedthroughs from hadronic decays such as $D^+ \rightarrow K^- \pi^+ \pi^+$ and $D^+ \rightarrow \pi^- \pi^+ \pi^+$ are removed explicitly by excluding candidates with either $K\pi\pi$ or $\pi\pi\pi$ invariant mass within $20 \text{ MeV}/c^2$ of the D^+ mass. Feedthrough from the Cabibbo-favored (CF) decay $D_s^+ \rightarrow \phi \ell^+ \nu_\ell$ followed by $\phi \rightarrow K^+ K^-$ is eliminated by excluding the region between 1.01 and $1.03 \text{ GeV}/c^2$ in the $K^+ K^-$ invariant mass.

In the rarer $D^+ \rightarrow \rho^0 \ell^+ \nu_\ell$ mode, additional selection criteria are required to reduce non-charm background and to eliminate feedthrough from the CF $D^+ \rightarrow \bar{K}^{*0} \ell^+ \nu_\ell$ mode, which has a rate 20 times larger. The following criteria, applied only to $D^+ \rightarrow \rho^0 \ell^+ \nu_\ell$, further reduce non-charm background. The maximal missing mass squared, $M_{miss}^2 = M_D^2 + M_{vis}^2 - 2M_D \sqrt{M_{vis}^2 + p_T^2}$, is required to be in the range -0.10 to $0.15 (\text{GeV}/c^2)^2$. The scalar sum of the transverse momenta of the daughter tracks with respect to the D^+ flight direction is required to be greater than $1.0 \text{ GeV}/c$. Although these quantities are partially correlated with the minimum parent mass, they do provide additional discriminating power.

When a K from the CF mode $D^+ \rightarrow \bar{K}^{*0} \ell^+ \nu_\ell$ is misidentified as a π , the reflected di-pion invariant mass is similar in position and shape to the ρ^0 resonance. It is thus imperative to reduce contamination from $D^+ \rightarrow \bar{K}^{*0} \ell^+ \nu_\ell$ to a level well below the signal. This is achieved with three selection criteria applied to candidate $D^+ \rightarrow \rho^0 \ell^+ \nu_\ell$ decays, but not to the normalizing mode. 1) The minimum parent mass computed for a $K\pi\ell\nu_\ell$ hypothesis, $M_{min}(K\pi\ell\nu_\ell)$, is required to be greater than $2.0 \text{ GeV}/c^2$. Monte Carlo studies show that less than 5% of observed $D^+ \rightarrow \bar{K}^{*0} \ell^+ \nu_\ell$ decays populate the $M_{min}(K\pi\ell\nu_\ell)$ distribution above $2.0 \text{ GeV}/c^2$, while about 70% of $D^+ \rightarrow \rho^0 \ell^+ \nu_\ell$ decays populate this region (when a pion is incorrectly assigned the mass of a kaon). 2) Information from the Čerenkov counters for both hadron candidates is used to reject about 51% of $K\pi$ pairs, yet keep about 92% of $\pi\pi$ pairs. 3) Although no significant K^* peak in $K\pi$ invariant mass remains after these requirements, the $K\pi$ mass for the hadrons is still required to be outside the interval 0.85 to $0.93 \text{ GeV}/c^2$. These three cuts combined with those described earlier result in a relative reduction factor of nearly 200 for the $D^+ \rightarrow \bar{K}^{*0} \ell^+ \nu_\ell$ mode compared with the $D^+ \rightarrow \rho^0 \ell^+ \nu_\ell$ mode.

Figures 1 and 2 show the signals in $D^+ \rightarrow \rho^0 \ell^+ \nu_\ell$ and the normalizing channel $D^+ \rightarrow \bar{K}^{*0} \ell^+ \nu_\ell$ for both the electronic and muonic modes. Simultaneous binned maximum likelihood fits to both the RS and WS distributions are performed separately for the electronic and muonic channels in both the $D^+ \rightarrow \rho^0 \ell^+ \nu_\ell$ and $D^+ \rightarrow \bar{K}^{*0} \ell^+ \nu_\ell$ decays. Two functions are used in the fit: a p-wave Breit-Wigner shape describes the ρ^0 signal and the function $F(M) = N_0(M - m_0)^\alpha \exp [c_1(M - m_0) + c_2(M - m_0)^2]$, where N_0 , m_0 , α , c_1 and c_2 are free parameters, characterizes the background under the ρ^0 (K^{*0}) peak in the RS sample which is assumed to have the same distribution as the WS sample. The normalizations for the RS background and the WS distribution are allowed to vary independently. In the case of $D^+ \rightarrow \rho^0 \ell^+ \nu_\ell$, the shape of the ρ^0 is modified by the energy available in the D^+ decay. Thus, the ρ^0 mass and width are taken from Monte Carlo simulation of the $D^+ \rightarrow \rho^0 \ell^+ \nu_\ell$ decay. For the $D^+ \rightarrow \bar{K}^{*0} \ell^+ \nu_\ell$ mode, both the K^{*0} width and peak position are free parameters in the fit; the values obtained from the fit agree with those from Monte Carlo. The p-wave Breit-Wigner functions from the fits are integrated from 0.65 to 0.90 GeV/ c^2 for the $\pi^+\pi^-$ invariant mass for the $D^+ \rightarrow \rho^0 \ell^+ \nu_\ell$ signal, and from 0.85 to 0.93 GeV/ c^2 for the $K\pi$ invariant mass for the $D^+ \rightarrow \bar{K}^{*0} \ell^+ \nu_\ell$ signal. The yields for both the $D^+ \rightarrow \rho^0 \ell^+ \nu_\ell$ and $D^+ \rightarrow \bar{K}^{*0} \ell^+ \nu_\ell$ channels are listed in Table I.

The efficiencies are factorized into two parts. The Čerenkov particle identification efficiencies are determined from a sample of $D^+ \rightarrow K^- \pi^+ \pi^+$ decays from real data, where the kaon and pions can be identified by charge alone. The rest of the reconstruction efficiencies and acceptances are determined from Monte Carlo simulation. Only the relative efficiencies for $D^+ \rightarrow \rho^0 \ell^+ \nu_\ell$ and $D^+ \rightarrow \bar{K}^{*0} \ell^+ \nu_\ell$ enter our final result. The overall efficiencies for the $D^+ \rightarrow \rho^0 \ell^+ \nu_\ell$ and $D^+ \rightarrow \bar{K}^{*0} \ell^+ \nu_\ell$ channels, as well as for the background modes, are listed in Table I.

Only backgrounds which populate the ρ^0 region and mimic the ρ^0 resonance are troublesome in the raw $D^+ \rightarrow \rho^0 \ell^+ \nu_\ell$ signal. Using simulated hadronic charm decays from the channels most likely to feed into $D^+ \rightarrow \rho^0 \ell^+ \nu_\ell$ signal, we found that hadronic charm decay feedthrough to the $D^+ \rightarrow \rho^0 \ell^+ \nu_\ell$ signal is negligible.

The background contributions to the signal mainly come from real semileptonic charm decays. The amount of feedthrough from them is based on efficiencies estimated from Monte Carlo studies and Particle Data Group (PDG) [8] branching ratios unless otherwise noted. To estimate the backgrounds from D_s^+ decays, the D_s^+ to D^+ production cross section ratio $\sigma_{D_s^+}/\sigma_{D^+}$ is needed. The weighted average of the measurements from hadronic charm production experiments [10] with a conservative error, 0.58 ± 0.15 , is used. The most significant semileptonic charm decay backgrounds are listed in Table I along with the corresponding estimated number of events in the $D^+ \rightarrow \rho^0 \ell^+ \nu_\ell$ signal. Requiring candidates to lie between 0.65 and 0.90 GeV/ c^2 in $\pi^+ \pi^-$ mass effectively removes decays from $D_s^+ \rightarrow \phi \ell^+ \nu_\ell$, $\phi \rightarrow K^+ K^-$, as well as from $D^+ \rightarrow \eta \ell^+ \nu_\ell$, $D_s^+ \rightarrow \eta \ell^+ \nu_\ell$. The contribution to the signal from these modes is negligible. The backgrounds from non-resonant or higher-mass-resonance decays are negligible as well.

After background subtraction, the final numbers of signal events are 49 ± 17 for $D^+ \rightarrow \rho^0 e^+ \nu_e$ and 54 ± 18 for $D^+ \rightarrow \rho^0 \mu^+ \nu_\mu$. The yields in the normalizing channels are 892 ± 52 for $D^+ \rightarrow \bar{K}^{*0} e^+ \nu_e$ and 769 ± 54 for $D^+ \rightarrow \bar{K}^{*0} \mu^+ \nu_\mu$.

Systematic errors associated with lepton identification are largely cancelled in the ratio of the $D^+ \rightarrow \rho^0 \ell^+ \nu_\ell$ and $D^+ \rightarrow \bar{K}^{*0} \ell^+ \nu_\ell$ decay rates. Remaining sources of systematic error are 1) uncertainties in the branching ratios used in background subtraction, 2) uncertainty in the D_s^+ to D^+ production cross section ratio $\sigma_{D_s^+}/\sigma_{D^+}$, 3) determination of relative efficiencies and 4) the fitting procedure. The uncertainties in the relative efficiencies are dominated by the momentum dependence of the Čerenkov identification and the dependence of the $D^+ \rightarrow \rho^0 \ell^+ \nu_\ell$ acceptances on the form factors. The effects of the uncertainties in the assumptions made in the fit are evaluated by varying the width of the ρ^0 peak and the shape of the background distribution. For the electronic channel, the four sources contribute approximately equally to the systematic error, each with a size about one third of the statistical error. For the muonic channel, the first three sources contribute approximately equally (about one third of the statistical error each) while the last source contributes an uncertainty about one sixth that of the statistical error. Further studies were performed to

search for other potential systematic effects by varying the selection criteria one at a time. No significant effects were found.

The rate for the decay $D \rightarrow V\ell^+\nu_\ell$, where V is a vector meson, is determined in the limit of massless ℓ by three form factors $A_1(q^2)$, $A_2(q^2)$ and $V(q^2)$, where q^2 is the square of the four-momentum transfer from D to V [11]. The present experimental information for $D^+ \rightarrow \bar{K}^{*0}\ell^+\nu_\ell$ decays is usually presented as $A_1(0)$, and the ratios of form factors $r_2(0) \equiv A_2(0)/A_1(0)$ and $r_V(0) \equiv V(0)/A_1(0)$, with an assumed q^2 dependence proportional to $(1 - q^2/M_p^2)^{-1}$ and $M_p \sim 2.1$ to 2.5 GeV/ c^2 . Since we have insufficient statistics in this experiment to measure the $D^+ \rightarrow \rho^0\ell^+\nu_\ell$ form factors, the simulations on which our efficiencies are based assumed $r_2(0) = 0.82$ and $r_V(0) = 2.0$, close to the present world averages [11] for $D^+ \rightarrow \bar{K}^{*0}\ell^+\nu_\ell$. We have checked the effect on the detection efficiency of significantly different values of the input r_2 and r_V . Specifically, assuming $r_2(0) = 0.0$ or $r_V(0) = 1.0$ changes our $D^+ \rightarrow \rho^0\ell^+\nu_\ell$ branching fraction by less than $(10 \pm 5)\%$ of itself. These variations have been included in the systematic uncertainty.

From the background-subtracted event yields and the efficiencies for $D^+ \rightarrow \rho^0\ell^+\nu_\ell$ and $D^+ \rightarrow \bar{K}^{*0}\ell^+\nu_\ell$ decays, the following branching ratios are determined:

$$\frac{\mathcal{B}(D^+ \rightarrow \rho^0 e^+ \nu_e)}{\mathcal{B}(D^+ \rightarrow \bar{K}^{*0} e^+ \nu_e)} = (4.5 \pm 1.4 \pm 0.9)\%,$$

$$\frac{\mathcal{B}(D^+ \rightarrow \rho^0 \mu^+ \nu_\mu)}{\mathcal{B}(D^+ \rightarrow \bar{K}^{*0} \mu^+ \nu_\mu)} = (5.1 \pm 1.5 \pm 0.9)\%.$$

We combine the results from the electronic and muonic modes, taking correlated errors into account, to obtain a final result of

$$\frac{\mathcal{B}(D^+ \rightarrow \rho^0 \ell^+ \nu_\ell)}{\mathcal{B}(D^+ \rightarrow \bar{K}^{*0} \ell^+ \nu_\ell)} = (4.7 \pm 1.3)\%,$$

where the error includes both statistical and systematic uncertainties. In Table II our result is compared with the only previously-published experimental result, from E653 [3], and various theoretical predictions. Our result, which is sensitive mainly to the form factor A_1 at $q^2 \approx 0.5$ (GeV/ c)², agrees only marginally with quark model predictions [9,12,13], but agrees well with recent lattice QCD calculations [14–17] and several other theoretical

predictions [18–20]. It thus begins to discriminate among models that are also used to predict form factors for $b \rightarrow u$ semileptonic decays to extract V_{ub} .

We gratefully acknowledge the assistance of the staffs of Fermilab and of all the participating institutions. This research was supported by the Brazilian Conselho Nacional de Desenvolvimento Científico e Tecnológico, CONACyT (Mexico), the Israeli Academy of Sciences and Humanities, the U.S. Department of Energy, the U.S.-Israel Binational Science Foundation, and the U.S. National Science Foundation. Fermilab is operated by the Universities Research Association, Inc., under contract with the United States Department of Energy.

REFERENCES

- [1] N. Isgur and M.B. Wise, Phys. Rev. D **42** (1990) 2388.
- [2] Mark III Collaboration, J. Adler *et al.*, Phys. Rev. Lett. **62** (1989) 1821; CLEO Collaboration, M.S. Alam *et al.*, Phys. Rev. Lett. **71** (1993) 1311; CLEO Collaboration, F. Butler *et al.*, Phys. Rev. D**52** (1995) 2656; Fermilab E687 Collaboration, P.L. Frabetti *et al.*, Fermilab-Pub-96/139-E, submitted to Phys. Lett. B.
- [3] Fermilab E653 Collaboration, K. Kodama *et al.*, Phys. Lett. B **316** (1993) 455.
- [4] J. A. Appel, Ann. Rev. Nucl. Part. Sci. **42** (1992) 367, and references therein; D. J. Summers *et al.*, Proceedings of the *XXVIIth* Rencontre de Moriond, Electroweak Interactions and Unified Theories, Les Arcs, France (15-22 March 1992) 417; S. Amato *et al.*, Nucl. Instrum. and Methods **A324** (1993) 535.
- [5] D. Bartlett *et al.*, Nucl. Instrum. and Methods **A260** (1987) 55.
- [6] V.K. Bharadwaj *et al.*, Nucl. Instrum. and Methods **A228** (1985) 283.
- [7] CLEO Collaboration, G. Brandenburg *et al.*, Phys. Rev. Lett. **75** (1995) 3804.
- [8] Particle Data Group, Phys. Rev. D**50** (1994) 1173.
- [9] N. Isgur, D. Scora, B. Grinstein and M.B. Wise, Phys. Rev. D **39** (1989) 799; D. Scora and N. Isgur, Phys. Rev. D**52** (1995) 2783.
- [10] ACCMOR Collaboration, S. Barlag *et al.*, Z. Phys. C**49** (1990) 555; Fermilab E653 Collaboration, K. Kodama *et al.*, Phys. Lett. B**309** (1993) 483; Fermilab E769 Collaboration, G.A. Alves *et al.*, Phys. Rev. Lett. **77** (1996) 2388.
- [11] J.D. Richman and P.R. Burchat, Rev. Mod. Phys. **67** (1995) 893.
- [12] W. Jaus, Phys. Rev. D**53** (1996) 1349.
- [13] M. Wirbel, B. Stech, and M. Bauer, Z. Phys. C**29** (1985) 637; M. Wirbel, Nucl. Phys.

- B (Proc. Suppl.) **13** (1990) 255.
- [14] A. Abada *et al.*, Nucl. Phys. B**416** (1994) 675.
- [15] C.R. Allton *et al.*, Phys. Lett. B**345** (1995) 513.
- [16] K.C. Bowler *et al.*, Phys. Rev. D**51** (1995) 4905.
- [17] V. Lubicz, G. Martinelli, M.S. McCarthy and C.T. Sachrajda, Phys. Lett. B**274** (1992) 415.
- [18] B. Bajc, S. Fajfer and R.J. Oakes, Phys. Rev. D**53** (1996) 4957.
- [19] R. Casalbuoni *et al.*, Phys. Lett. B**299** (1993) 139.
- [20] P. Ball, Phys. Rev. D**48** (1993) 3190.

TABLES

TABLE I. Numbers of $D^+ \rightarrow \rho^0 \ell^+ \nu_\ell$ and $D^+ \rightarrow \bar{K}^{*0} \ell^+ \nu_\ell$ signal events from the fit to the data, estimated numbers of background events, efficiencies \mathcal{E} for each decay mode and input to the calculation of backgrounds. Efficiencies include branching ratios for non-charm decays.

Decay	ℓ	# of events	$\mathcal{E}(\%)$	Input
Raw $\rho^0 \ell \nu_\ell$ signal	μ	81.3 ± 16.6		Fit results, before
	e	73.9 ± 15.2		background subtraction
$D_s^+ \rightarrow \eta' \ell^+ \nu_\ell$	μ	15.1 ± 6.4	0.073	CLEO measurement [7] for
$\hookrightarrow \gamma \rho, \gamma \omega$	e	14.2 ± 6.0	0.064	$\mathcal{B}(D_s^+ \rightarrow \eta' \ell^+ \nu_\ell) / \mathcal{B}(D_s^+ \rightarrow \phi \ell^+ \nu_\ell)$
$D^+ \rightarrow \bar{K}^{*0} \ell^+ \nu_\ell$	μ	4.1 ± 1.5	0.001	PDG [8] branching ratios
$\rightsquigarrow \text{“}\pi^- \text{”} \pi^+$	e	3.6 ± 1.1	0.001	
$D_s^+ \rightarrow \phi \ell^+ \nu_\ell$	μ	3.7 ± 1.3	0.017	PDG [8] branching ratios
$\hookrightarrow \rho \pi, \pi^+ \pi^- \pi^0$	e	3.5 ± 1.2	0.014	
$D^+ \rightarrow \eta' \ell^+ \nu_\ell$	μ	2.9 ± 1.2	0.088	ISGW2 [9] prediction for
$\hookrightarrow \gamma \rho, \gamma \omega$	e	2.1 ± 1.2	0.062	$\mathcal{B}(D^+ \rightarrow \eta' \ell^+ \nu_\ell) / \mathcal{B}(D^+ \rightarrow \rho^0 \ell^+ \nu_\ell)$
$D^+ \rightarrow \omega \ell^+ \nu_\ell$	μ	1.2 ± 0.3	0.005	ISGW2 [9] prediction for
$\hookrightarrow \pi^+ \pi^- \pi^0, \pi^+ \pi^-$	e	1.1 ± 0.4	0.004	$\mathcal{B}(D^+ \rightarrow \omega \ell^+ \nu_\ell) / \mathcal{B}(D^+ \rightarrow \rho^0 \ell^+ \nu_\ell)$
$D^+ \rightarrow \rho^0 \ell^+ \nu_\ell$	μ	54 ± 18	0.19	Background subtracted signal
$\hookrightarrow \pi^+ \pi^-$	e	49 ± 17	0.16	
Normalizing mode				
$D^+ \rightarrow \bar{K}^{*0} \ell^+ \nu_\ell$	μ	769 ± 54	0.19	Fit results for
$\hookrightarrow K^- \pi^+$	e	892 ± 52	0.19	normalizing signals

TABLE II. Comparison of our results with the only previously-published experimental result and theoretical predictions. The PDG [8] branching ratio for $D^+ \rightarrow \bar{K}^{*0} \ell^+ \nu_\ell$ and D^+ lifetime are used to calculate the experimental decay rate for $D^+ \rightarrow \rho^0 \ell^+ \nu_\ell$. Most theoretical results are calculated for D^0 decays. To compare these results for D^0 decay with the experimental results for D^+ decay we use the relations $\Gamma(D^+ \rightarrow \bar{K}^{*0} \ell^+ \nu_\ell) = \Gamma(D^0 \rightarrow K^{*-} \ell^+ \nu_\ell)$ and $\Gamma(D^+ \rightarrow \rho^0 \ell^+ \nu_\ell) = 1/2 \times \Gamma(D^0 \rightarrow \rho^- \ell^+ \nu_\ell)$, where the factor of 2 difference between the two decay rates arises from the $1/\sqrt{2}$ coupling of $d\bar{d}$ to the ρ^0 . The second column indicates the method used to obtain the results, where QM stands for quark model, HQET for heavy quark effective theory, SR for QCD sum rule, and LQCD for lattice QCD.

Group	Method	ℓ	$\frac{\Gamma(D^+ \rightarrow \rho^0 \ell^+ \nu_\ell)}{\Gamma(D^+ \rightarrow \bar{K}^{*0} \ell^+ \nu_\ell)}$	$\Gamma(D^+ \rightarrow \rho^0 \ell^+ \nu_\ell) (10^{10} s^{-1})$
E791(this work)	Exp.	e	$0.045 \pm 0.014 \pm 0.009$	$0.20 \pm 0.07 \pm 0.05$
E791(this work)	Exp.	μ	$0.051 \pm 0.015 \pm 0.009$	$0.22 \pm 0.07 \pm 0.05$
E791(this work)	Exp.	ℓ	0.047 ± 0.013	0.21 ± 0.06
E653 [3]	Exp.	μ	$0.044_{-0.025}^{+0.031} \pm 0.014$	$0.19_{-0.11}^{+0.14} \pm 0.07$
ISGW2 [9]	QM	ℓ	0.022	0.12
Jaus [12]	QM	ℓ	0.030	0.33
Bajc [18]	HQET	ℓ	—	0.21 ± 0.02
			$\frac{1}{2} \frac{\Gamma(D^0 \rightarrow \rho^- \ell^+ \nu_\ell)}{\Gamma(D^0 \rightarrow K^{*-} \ell^+ \nu_\ell)}$	$\frac{1}{2} \Gamma(D^0 \rightarrow \rho^- \ell^+ \nu_\ell) (10^{10} s^{-1})$
BSW [13]	QM	ℓ	0.037	0.35
ELC [14]	LQCD	ℓ	0.047 ± 0.032	$0.3 \pm 0.15 \pm 0.05$
APE [15]	LQCD	ℓ	0.043 ± 0.018	0.3 ± 0.1
UKQCD [16]	LQCD	ℓ	$0.036_{-0.013}^{+0.010}$	0.215 ± 0.055
LMMS [17]	LQCD	ℓ	0.040 ± 0.011	0.20 ± 0.045
Casalbuoni [19]	HQET	ℓ	0.06	0.225
Ball [20]	SR	ℓ	—	0.12 ± 0.035

FIGURES

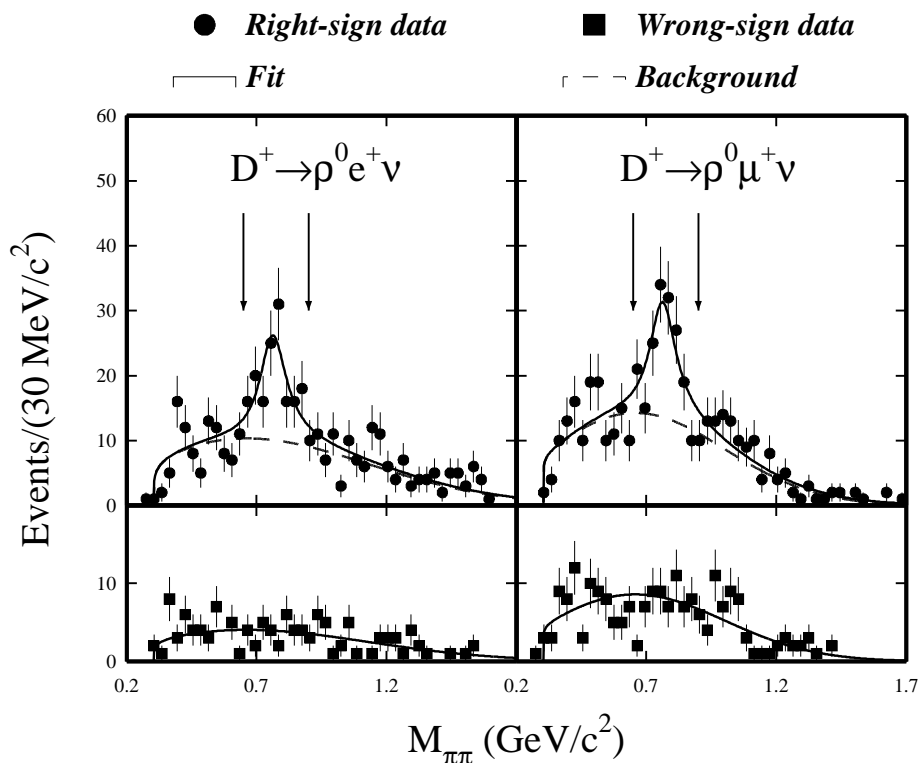


FIG. 1. $M_{\pi\pi}$ distribution for $D^+ \rightarrow \rho^0 \ell^+ \nu_\ell$ candidates. The vertical arrows indicate the mass window for the final $D^+ \rightarrow \rho^0 \ell^+ \nu_\ell$ candidates. For each leptonic mode, a simultaneous fit is made to the RS and WS data. The shape for the background distribution in the RS data is constrained to be the same as that of WS distribution, but the relative normalization is allowed to vary.

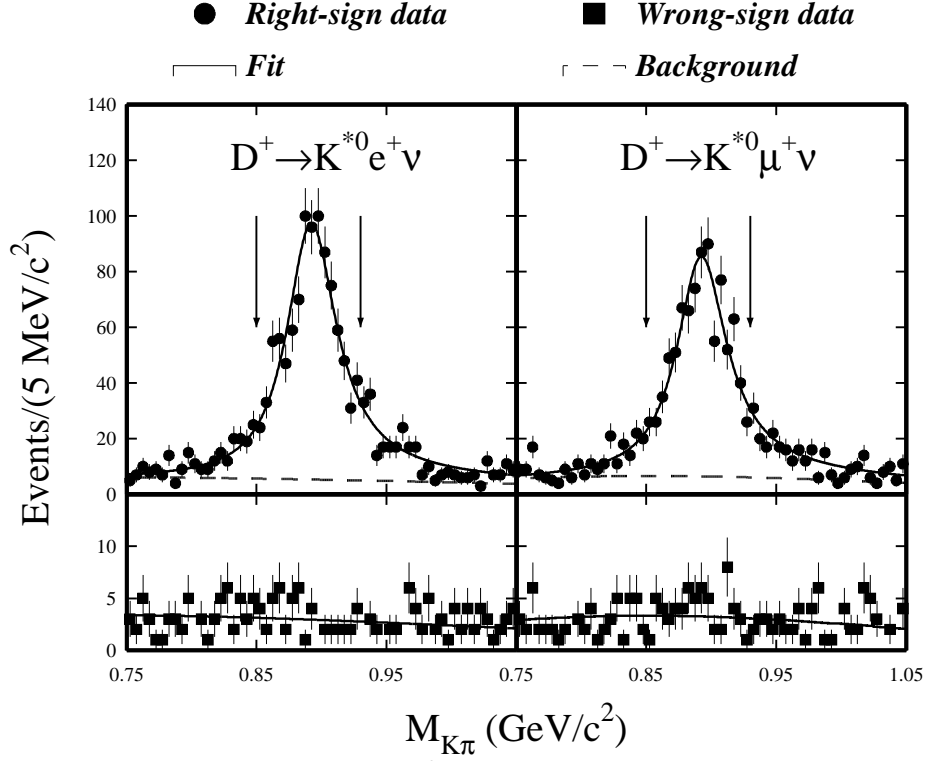


FIG. 2. $M_{K\pi}$ distribution for $D^+ \rightarrow \bar{K}^{*0} \ell^+ \nu_\ell$ candidates. The vertical arrows indicate the mass window for the final $D^+ \rightarrow \bar{K}^{*0} \ell^+ \nu_\ell$ candidates. For each leptonic mode, a simultaneous fit is made to the RS and WS data. The shape for the background distribution in the RS data is constrained to be the same as that of WS distribution, but the relative normalization is allowed to vary.